THE ELECTRICAL AND STRUCTURAL PROPERTIES OF ALUMINIUM AND NITROGEN DOPED ZINC OXIDE THIN FILM PREPARED BY RADIO FREQUENCY SPUTTERING

LOW LYNN YIEN

UNIVERSITI SAINS MALAYSIA

2013

THE ELECTRICAL AND STRUCTURAL PROPERTIES OF ALUMINIUM AND NITROGEN DOPED ZINC OXIDE THIN FILM PREPARED BY RADIO FREQUENCY SPUTTERING

By

LOW LYNN YIEN

Thesis submitted in fulfillment of the requirements

for the degree of

Master of Science

MAY 2013

ACKNOWLEDGEMENTS

First of all, thanksgiving my supervisor Professor Dr. Mat Johar Bin Abdullah, with his continuous guidance, advises and support throughout the whole experiment and the published works. I feel appreciate and happy to work as one of the member in his group.

I feel greatly thankful to all the laboratory staffs in N.O.R. lab and solid-state lab, because of their patience and generous help on the technical part during my research work. I would also like to offer my regards to the FE-SEM laboratory staff at the School of Biology and to all my colleagues in school of physics who assisted and accompanied me for these two years.

In addition, I appreciated the financial support from MOSTI to allow me finish my studies and also the research grant (RU-PRGS) from RCMO to give me the chance in carried out my research work.

Lastly sincere thanks to my family members and my friends on behalf of their infinite encouragement and supportive actions along my studies life.

Low Lynn Yien

TABLE OF CONTENTS

LIST OF FIGURES

LIST OF TABLES

LIST OF ABBREVIATIONS

AC	Alternating current
Ag	Silver
Al	Aluminium
ANZO	Aluminium-nitrogen codoped zinc oxide
Ar	Argon gas
As	Arsenic
AZO	Aluminium doped zinc oxide
Be	Beryllium
Cu	Copper
C-V	Capacitance-voltage
DC	Direct current
ECR	Electron cyclotron resonance
EDX	Energy dispersive X-ray spectroscopy
FESEM	Field Emission Scanning Electron Microscope
Ga	Gallium
GaN	Gallium nitride
H	Hydrogen
He	Helium
In	Indium
IR	Infrared
ITO	Indium tin oxide
I-V	Current-voltage
LaB6	Lanthanum Hexaboride
LD	Laser diode
LED	Light emitting diode
Li	Lithium
Mo	Molybdenum
MOS	Metal oxide semiconductor
N	Nitrogen
N_2	Nitrogen gas
N_2O	Nitrous oxide
Na	Natrium
NH_3	Ammonia
NO	Nitrogen monoxide
NO_2	Nitrogen dioxide
NZO	Nitrogen doped zinc oxide
O	Oxygen

P	Phosphorus
PEMOCVD	Plasma enhanced metal organic chemical vapour deposition
PLD	Pulsed laser deposition
P-MBE	Plasma asisted molecular beam epitaxial
PVD	Physical vapour deposition
RF	Radio frequency
RT	Room temperature
SEM	Scanning Electron Microscope
SiC	Silicon carbide
TCO	Transparent conductive oxide
USP	Ultrasonic spray pyrolysis
UV	Ultraviolet
UV-Vis	Ultraviolet–visible spectroscopy
W	Tungsten
XRD	X-ray diffraction
Zn	Zinc
ZnO	Undoped zinc oxide
ZnSe	Zinc selenide

LIST OF SYMBOLS

$(N_2)_i$	Nitrogen molecules in interstitial site defects
$(N_2)_O$	Nitrogen molecules in oxygen antisite defects
A	Gate area
L	Geometry sample length
a	Lattice constants in a-axis
a_0	Lattice constant in a plane at ambient condition (unstrained)
Abs	Absorbance
As_{Zn}	Arsenic in zinc antisite defects
at%	Atomic percentage
B	Full width at half maximum (FWHM)
b_0	Lattice constant in b plane at ambient condition (unstrained)
B_z	Magnetic field aplied in z direction
C	Geometry contact length
c_0	Lattice constant in c plane at ambient condition (unstrained)
C_{HF}	High frequency capacitance
C_{ij}	Elastic stiffness constants
c_{light}	Speed of light in vacuum
C_{max}	Maximum capacitance
C_{min}	Minimum capacitance
C_{ox}	Oxide capacitance
C_{QS}	Quasi-static/low frequency capacitance
D	Crystallite size
d_{hkl}	Interplanar spacing of a crystalline material in the plane of (hkl)
E_g	Optical band gap energy
E_p	Photon energy
eV	Electron volt
E_x	Electric field in the x direction
E_y	Electric field in the y direction
F	Geometrical factor
f_o	Frequency
H	Planck's constant
I	Current
I	Intensity of the sample beam
I_0	Intensity of the reference beam

I_{AC}	AC current
I_o	Current amplitude
k	Constant
k_B	Boltzmann constant
Li_{Zn}	Lithium in zinc antisite defects
L_s	Length of the semiconductor
m_0	Electron rest mass
m_e	Effective hole mass
m_h	Effective electron mass
N	Whole number
N_a	Space charge concentration
N_c	Effective density of states in conduction band
n_i	Intrinsic carrier concentration
n_n	Carrier concentration for electrons
n_p	Carrier concentration for holes
N_v	Effective density of states in valence band
℃	Degree celcius
O_i	Oxygen interstitial
P_{Zn}	Phosphorus in zinc antisite defects
q	Carrier charges
Q	Resistance ratio
R	Resistance
R_H	Hall coefficient
T_i	Transmittance
T	Temperature
t_{ox}	Oxide thickness
T_s	Substrate temperature
t_s	Thickness of the semiconductor
V	Potential difference/voltage
V_{AC}	AC voltage
V_{FB}	Flatband voltage
V_{GB}	Metal gate DC voltage
V_H	Hall voltage
$V_{ij,kl}$	Voltage drop measured between contacts k and l when the current is passing from contact i to j
$V^{-}_{ij,kl}$	Hall voltage of $V_{ij,kl}$ at negative magnetic field B_{-z}
$V^{+}_{ij,kl}$	Hall voltage of $V_{ij,kl}$ at positive magnetic field B_{+z}

V_O	Oxygen vacancy
V_o	Voltage amplitude
ν_p	Photon frequency
V_T	Threshold voltage
V_{Zn}	Zinc vacancy
W	Geometry sample width
w_s	Width of the semiconductor
wt%	Weight percentage
Z	Impedance
Z_C	Capacitance impedance
Zn_i	Zinc interstitial
Z_o	Impedance amplitude
Z_R	Resistance impedance
A	Absorption coefficient
ε_{ox}	Permittivity of the oxide
ε_s	Permittivity of the semiconductor
Θ	Bragg's angle
Λ	Wavelength of the X-ray source
λ_p	Photon wavelength
μ_n	Carrier mobility for electrons
μ_p	Carrier mobility for holes
P	Bulk resistivity
$\sigma_{(002)}$	Lattice stress in the (002) plane
Φ	Phase shift angle
ϕ_m	Metal work function
ϕ_s	Semiconductor work function
Ω	Angular frequency
$\vec{F}_{Lorentz}$	Lorentz force
$\vec{B}$	Magnetic field in vector
$\vec{v}$	Velocity of the carrier charges in vector

SIFAT-SIFAT ELEKTRIK DAN STRUKTUR BAGI FILEM NIPIS ZINK OKSIDA TERDOP ALUMINIUM DAN NITROGEN DISEDIAKAN SECARA PERCIKAN FREQUENSI RADIO

ABSTRAK

Zink Oksida (ZnO) adalah semikonduktor menarik untuk pelbagai aplikasi kerana jurang tenaga lebar dan langsung (3.37 eV) dengan tenaga mengikat exiton yang tinggi (60 MeV). Oleh itu, realisasi bagi penghasilan ZnO jenis-p yang baik adalah penting untuk pembentukan simpang homo p-n dalam peranti elektronik dan optoelektronik. Walau bagaimanapun, ZnO mempamerkan kekonduksian intrinsik jenis-n, keterlarutan pendopan jenis p yang rendah dan kesan pampasan yang menghalang penyelidikan terhadap bahan dan pembangunan peranti. Objektif utama kerja penyelidikan ini ialah untuk fabrikasi ZnO jenis-p berkualiti tinggi menggunakan pendekatan baru dalam persekitaran pertumbuhan kaya oksigen (O) secara percikan Frequensi Radio. Sifat-sifat struktur, elektrik dan optik filem ZnO yang difabrikasi telah dicirikan. Filem nipis ZnO terdop penerima di atas substrat kaca difabrikasikan secara percikan Frequensi Radio dari target ZnO dalam persekitaran gas N_2O/Ar. Perubahan suhu substrat (suhu bilik ke 400 ℃) dan nisbah gas N_2O (0 - 70%) digunakan untuk menentukan pembolehubah proces yang optimum bagi pemendapan ZnO terdop nitrogen (NZO) jenis p. Target aluminium (Al) dengan kuasa RF yang berbeza (0 – 110 W) digunakan untuk pemendapan filem nipis ZnO terdop aluminium dan nitrogen (ANZO) pada kepekatan Al yang berbeza untuk perbandingan dengan pendopan tunggal ZnO. Unsur kimia, morfologi dan

sifat-sifat struktur bagi filem yang disediakan dicirikan oleh spektroskopi sebaran elektron sinar-X (EDX), mikroskop imbasan elektron pancaran medan (FESEM) dan pembelauan sinar-X (XRD). Sifat-sifat optik dicirikan oleh spektroskopi ultralembayung nampak (UV-Vis), manakala sifat-sifat elektrik diukur dengan sistem pengukuran kesan Hall buatan sendiri. Di samping itu, pengukuran kapasitan-voltan (*C-V*) bagi struktur semikonduktor-oksida-logam (MOS) telah dilakukan untuk mengesahkan keputusan pengukuran Kesan Hall. Filem nipis ZnO jenis-p yang seragam dengan struktur yang cenderung berorientasikan (002) telah dihasilkan melalui penekanan kecacatan penderma asal. Suhu substrat, nisbah N_2O% dan kepekatan Al didapati mempengaruh jenis kekonduksian filem ZnO yang difabrikasikan. Pengukuran *C-V* dan kesan Hall mededahkan kehadiran sebilangan besar kecacatan dan pendopan yang tidak aktif dalam filem yang disediakan. Walau bagaimanapun, melalui kaedah pendopan bersama Al-N, keterlarutan N telah meningkat dan lebih banyak pendopan jenis-p dapat diaktifkan. Filem nipis ZnO jenis-p yang terbaik mempunyai kerintangan sebanyak 0.4 Ω.cm dan ketumpatan lubang setinggi 4.2×10^{19} cm^{-3}, telah dicapai pada suhu bilik dengan nisbah gas 30% N_2O dan 0.5 at% Al; namun, kualiti hablur dan mobiliti lubang bagi filem berkenaan telah merosot berbanding filem-filem lain. Mekanisme bagi pembentukan jenis pembawa dominan dalam filem dibincangkan berdasarkan keputusan yang diperolehi.

THE ELECTRICAL AND STRUCTURAL PROPERTIES OF ALUMINIUM AND NITROGEN DOPED ZINC OXIDE THIN FILM PREPARED BY RADIO FREQUENCY SPUTTERING

ABSTRACT

Zinc Oxide (ZnO) is an attractive semiconductor for various applications due to its direct wide band gap (3.37 eV) and high exciton binding energy (60 meV). Thus, realization of reproducible and good p-type ZnO is important for the formation of homo p-n junction in electronic and opto-electronic devices. However, ZnO exhibits intrinsic n-type conductivity, low acceptors solubility and compensation effect that have hindered research on the materials and device development. The main objective of this research work is to fabricate high quality p-type ZnO using a new approach in an oxygen (O) rich growth environment by RF magnetron sputtering. The structural, electrical and optical properties of the fabricated ZnO film were characterized. The acceptor doped ZnO thin films on glass substrate were fabricated by the RF sputtering of ZnO target in N_2O/Ar gas environment. The variation of substrate temperature (room temperature to 400 ℃) and gas ratio of N_2O (0 - 70%) were applied in order to determine the optimum process variables for the deposition of p-type nitrogen doped ZnO (NZO). Aluminium (Al) metal target with different RF power (0 – 110 W) was used for the deposition of aluminium and nitrogen doped ZnO (ANZO) thin films at different Al concentration in order to compare with single doped ZnO. The chemical element, morphology and structural properties of the prepared films were characterized by electron dispersive X-ray spectroscopy (EDX), field emission scanning electron microscope (FESEM) and X-ray diffraction (XRD).

The optical properties were characterized by ultraviolet-visible spectroscopy (UV-Vis), while the electrical properties were measured by a homemade Hall Effect measurement system. In addition, capacitance-voltage (*C-V*) measurement on metal-oxide-semiconductor (MOS) structure based on ZnO films was performed to verify the results of Hall Effect measurement. Uniform p-type ZnO thin film with (002) plane preferred orientation was realized through suppression of native donor defects. Substrate temperature, N_2O% ratio and Al concentration were found to influence the conductivity type of the fabricated ZnO films. *C-V* and Hall Effect measurements revealed the presence of large number of defects and inactive dopants in the prepared films. However through Al-N codoping method the N solubility had been increased and more acceptors had been activated. The best p-type ZnO thin film with resistivity of 0.4 Ω.cm and high holes concentration of 4.2×10^{19} cm^{-3} was achieved at room temperature with 30% N_2O gas ratio and 0.5at% of Al; however, the film's crystalline quality and the carrier mobility have been degraded as compared to other films. The mechanisms for the formation of the dominant carrier type in the films were discussed based on the obtained results.

CHAPTER 1: INTRODUCTION TO ZINC OXIDE

1.1 Fundamental properties of zinc oxide (ZnO)

Zinc oxide (ZnO) known as zincite is the naturally oxide compound for zinc (Zn) element. It is a low cost, relatively abundant and non-toxic material [1]. This wide band gap (~3.37 eV) II-VI compound semiconductor naturally possesses the hexagonal wurtzite crystal structure, where one Zn ion is tetrahedral surrounded by four oxygen ions (O) and vice-versa [2], as shown in Figure 1.1. The lattice constant for the hexagonal wurtzite crystal structure at ambient condition is $a_0 = b_0 = 0.3249$ nm and $c_0 = 0.5207$ nm. Other than wurtzite structure, ZnO can be also stably grown in zincblende [Figure 1.2(a)] structure on a suitable cubic substrate or a rocksalt [Figure 1.2(b)] structure at relatively high pressure. The ionicity of ZnO resides at the borderline between the covalent and ionic semiconductors [3]. Table 1.1 shows the basic physical properties of ZnO.

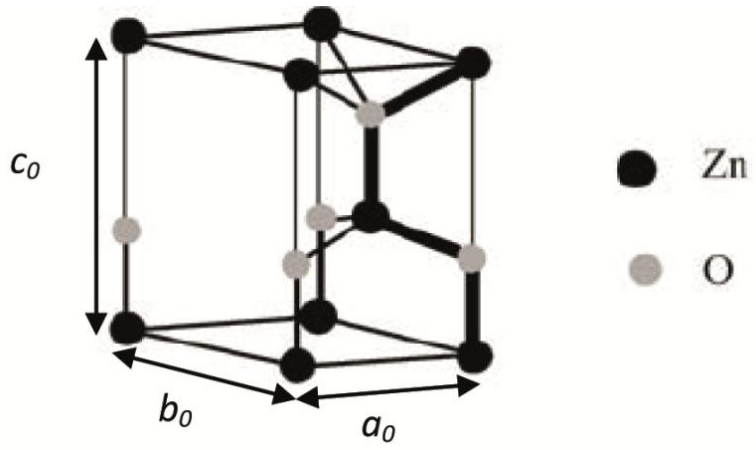

Figure 1.1 Hexagonal wurtzite structure of ZnO with lattice parameters at ambient condition, where $a_0 = b_0 \neq c_0$. [3]

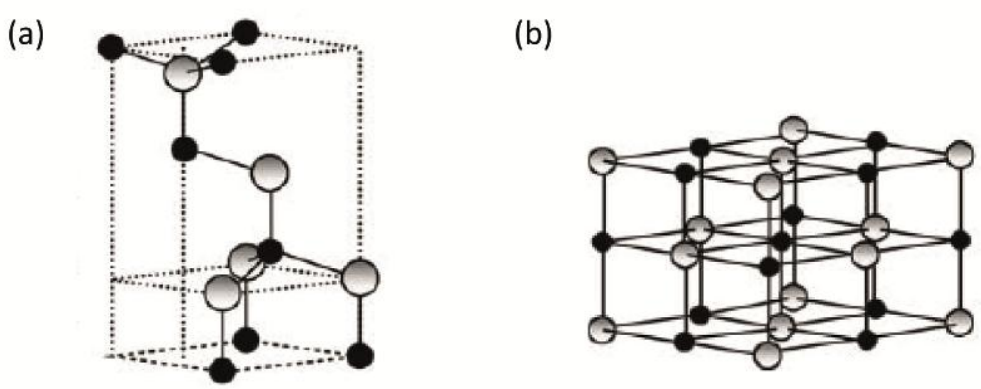

Figure 1.2(a) Zincblende cubic structure and (b) rocksalt cubic structure. [3]

Table 1.1 The basic physical properties of ZnO. [4]

Property	Value
Lattice parameters at 300 K (nm)	a_0: 0.32495 c_0: 0.52069
Density (g cm^{-3})	5.606
Stable phase at 300 K	Wurtzite
Melting point (°C)	1975
Thermal conductivity	0.6, 1-1.2
Linear thermal expansion coefficient	a_0: 6.5×10^{-6} c_0: 3.0×10^{-6}
Static dielectric constant	8.656
Refractive index	2.008, 2.029
Energy bandgap (eV)	Direct, 3.37
Intrinsic carrier concentration (cm^{-3})	$<10^6$ max n-type doping: $n \sim 10^{20}$ max p-type doping: $p \sim 10^{17}$
Exciton binding energy (meV)	60
Electron effective mass	0.24
Electron Hall mobility, n-type at 300 K ($cm^2V^{-1}s^{-1}$)	200
Hole effective mass	0.59
Hole Hall mobility, p-type at 300 K ($cm^2V^{-1}s^{-1}$)	5 - 50

1.2 Importance of ZnO

ZnO has been discovered long ago to be used in commercial application. Due to the high refractivity and chemical stability, ZnO powder has been used as white

pigment over 200 years. It has been used as an agriculture stabilizer to offset a lack of zinc in soil and to use as the mineral ingredient for many cosmetic products [5]. In the beginning of the semiconductor age after the invention of the transistors, ZnO has been found to show good piezoelectric behavior [1]. Since then, ZnO is emerging as a material of interest for electronic application, such as the varistors and other voltage limiting devices [6], transducer [7] and surface wave acoustic devices [8]. Highly transparent in the visible spectral region and electrically conductive of ZnO has also makes it a viable material for lower cost transparent conductive coating (TCO) as compared to indium tin oxide (ITO), which can be use for variety of devices such as solar cell [9] and flat panel displays [10].

The need for short-wavelength, high-power optoelectronic devices have stimulated the research on wide band gap materials. These included ZnO, gallium nitride (GaN), zinc selenide (ZnSe) and 6H-Silicon carbide (SiC) with their related properties are shown in Table 1.2.

Table 1.2 Crystal structure, lattice parameters and energy band gap of various wide band gap semiconductors as comparison. [11]

Material	**Crystal Structure**	**Lattice constant**		**Energy band gap, E_g (eV)**
		a_0 **(nm)**	c_0 **(nm)**	
ZnO	Wurtzite	0.3249	0.5207	3.37
GaN	Wurtzite	0.3189	0.5185	3.39
ZnSe	Zincblende	0.3823	-	2.70
6H-SiC	Wurtzite	0.3081	1.512	2.86

So far, GaN is the predominant material for optoelectronic devices as compared to ZnSe because ZnSe forms defects under high current application and 6H-SiC which is an indirect band gap semiconductor [12]. The triggered of interest on ZnO for optoelectronic application begin from the realization of p-type ZnO, where p-n

homojunction is expected to have better performance than heterojunction. ZnO has large exciton binding energy of 60 meV which is much higher than the effective thermal energy at room temperature (26 meV). Thus, lasing action based on excitonic gain mechanism at room temperature can be expected on ZnO based optoelectronic devices [1]. Several potential advantages of ZnO over the GaN are 2.4 times larger exciton binding energy than that of GaN, availability to be grown in high quality bulk, and ease of wet chemical etching process. Hence, ZnO is favored as a potential competitor in blue or ultraviolet (UV) range based optoelectronic devices such as light emitting diode (LED) [13] and laser diode (LD) [14].

1.3 Doping in ZnO

High quality of both n-type and p-type materials are necessary for the development of ZnO based optoelectronic devices. However, the deviation from stoichiometry to either side of donors or acceptors is the main problem for wide band gap semiconductor. In the case of ZnO, it is naturally n-type due to the asymmetry doping caused by the native defects.

The main defects in the ZnO films are mainly vacancies (Atom is missing from its regular atomic site), interstitial (high energy or smaller size atoms that reside in the non-atom lattice site) and antisite (occur in an ordered alloy or compound where different type of atoms exchange its positions with each other). [15]

In details, oxygen vacancy (V_o) and zinc interstitial (Zn_i) are the main native defects which acting as shallow donors in ZnO. While the formation of acceptors

native defects such as oxygen interstitial (O_i) and zinc vacancy (V_{Zn}) is very rare due to the high formation enthalpies in zinc rich growth condition [16, 17].

Hydrogen (H) impurity and its related compound which is believed to act as a shallow donor in the ZnO lattice is also one of the reasons for n-type conduction [18], where there were some reports on the rapid and deep diffusion of H into the ZnO [19, 20], the removal of H related compound by thermal annealing to obtain p-type ZnO [21-23]. However, the unintentionally presence of H in ZnO is mostly found on the chemical vapour or water vapour deposition method.

The n-type conductivity of ZnO can be easily enhanced and reproduced by doping with the group III elements such as aluminum (Al), gallium (Ga) and indium (In) [24-26]. These substitutional elements for Zn can help to obtain metal-like ZnO thin film ($\rho > 10^{-4}\ \Omega$.cm) with high electron concentration ($>10^{20}\ cm^{-3}$) easily, where Shin et al. [27] reported a minimum resistivity of $3.72 \times 10^{-4}\ \Omega$.cm and carrier concentration of $2.33 \times 10^{21}\ cm^{-3}$ at Ga composition of 5 wt% and substrate temperature, T_s of 300 ℃.

1.4 Problem statement for ZnO

Although there was a rapid development in ZnO films, the major obstacle for ZnO-based optoelectronic devices is the difficulty in fabricating p-type films. Many effort have been done on p-type but there is still a need to produce good-quality and reproducible p-type material. The difficulty in getting p-type is due to the compensation effects of donor defects, deep acceptors level and low acceptors solubility limit.

1.5 Research Objective

The main objective of this research is to fabricate high quality and reproducible p-type ZnO by RF magnetron sputtering technique, followed by the electrical, structural and optical studies of these films.

- A new approach is taken whereby N_2O/Ar gas will be introduced in the sputtering of ZnO in order to create O rich growth condition that could suppress the formation of native donors such as Zn_i and V_O. The effect of introducing different concentration (0 - 70%) of N_2O gas into the growth chamber for nitrogen doped ZnO (NZO) thin films will be investigated.
- Present work will be focused on lower temperature fabrication (< 450 ℃) to avoid the escape of N from the film. The substrate temperature for the deposition of NZO thin films will be varied from room temperature (RT) to 400 ℃.
- In order to enhance the p-type conductivity, aluminium-nitrogen codoped ZnO (ANZO) thin films will be fabricated. The power on aluminium (Al) metal target will be carefully controlled to incorporate different concentration (0 – 0.9 at %) of Al into the film.
- Possible conduction mechanism involved in the undoped and doped zinc oxide (ZnO) films will be compared and determined by structural, electrical and optical characterizations.
- Capacitance-voltage (*C*-*V*) measurement on metal-oxide-semiconductor (MOS) structure will be carried out to confirm the carrier type of the prepared ZnO films since it is a powerful technique available and only a few works have been reported in the literature.

1.6 Thesis Outline

Chapter 1 provides the fundamental properties, application and doping in ZnO. This chapter also introduced some of the bottlenecks in obtaining p-type conductivity and objective of our work. Where else, **Chapter 2** encloses the literature review for p-type ZnO, theoretical background as well as the formulae for the growth and the characterization techniques on ZnO. **Chapter 3** contains the experimental details and flow chart for ZnO samples preparation. Continue with **Chapter 4** covered the parts for electrical, structural and optical results with their related discussion. **Chapter 5** deals with the research conclusions and the proposal for the future work in order to improve the current work.

CHAPTER 2: LITERATURE REVIEW AND THEORITICAL BACKGROUND

2.1 Literature review on p-type ZnO

Calculations by Oba et al. [17] suggest that the native donor defects mentioned in the section 1.3 have low formation enthalpies in both the zinc-rich and oxygen-rich condition, which will effectively compensate p-type doping. Although group I elements such as lithium (Li), natrium (Na) and silver (Ag) acceptors has been proposed, substitution of Zn by group I element such as Li (Li_{Zn}) is found to be a deep acceptors with the level as high as 800 meV [28]. Moreover, p-type can be achieved only at the optimal concentrations of 0.6 at% Li, otherwise high-resistivity ZnO was obtained when Li concentration was more than 1.2 at% [29]. Group V elements such as nitrogen (N), phosphorus (P) and arsenic (As) are also known to be the acceptors for ZnO. According to Park et al. [30], much larger ionic radius of P and As was found to be deep acceptors and difficult to dope at O sites, which led to the formation of donor-like anti-site of *AX* centre. Although P and As are amphoteric, they also have a tendency to form P at Zn anti-sites (P_{Zn}) and As at Zn anti-sites (As_{Zn}), which are also donors.

Limitation and uncertainty in electrical characterization has also made the determination of p-type ZnO becomes difficult. Hall Effect measurement is the most straight forward and common technique to determine the type of conduction, whereby it will show p-type when the condition of $n_p\mu_p^2 > n_n\mu_n^2$ is fulfilled [31, 32]. Unfortunately, incorrect conductivity type on ZnO by Hall Effect measurement was usually observed and discussed by few researchers [33-35]. The reason for this includes the inhomogeneous of films, lack of symmetry in contacts placement and

also due to the dependent of Hall result on the carrier mobility; the very small Hall voltages of p-type due to the low hole mobility can cause the uncertainty in the conduction type. Thus, error must be eliminated to obtain an accurate type of conduction. Hence, the theory and calculation of Hall measurement will be discussed in the section 2.5.

Although Lyons et al. [36] suggested that N (group V element) has a very deep acceptors level that could not led to the p-type conduction, it is still believed that N remained the most suitable dopants for p-type due to the high formation energy as an *AX* anti-site donor defects, has similar ionic size with O and has the highest solubility limit among the other acceptors [31]. There are a few types of N source such as nitrogen gas (N_2), nitrous oxide (N_2O), nitrogen monoxide (NO), nitrogen dioxide (NO_2) and ammonia (NH_3). N_2O is more likely to be chosen among these sources because it is non-toxic as compared to NO_2 and NO which led to safer and cost saving without the need of toxic processing system. It also eliminates the possibility of the unintentionally incorporation of H source (NH_3) as donors into the ZnO. Furthermore, N_2O has lower ionization energy (12.89 eV) compared to nitrogen gas N_2 (15.58 eV) which helps to obtained N acceptors more easily with plasma [37]. In high nitrogen gas (N_2) concentration, it is difficult to break the triple bond between N_2 even with plasma introduced, hence the N-N substitution in oxygen sites [$(N_2)_O$] or interstitial sites [$(N_2)_i$] with lower formation energy is introduced, which act as a double shallow donor in compensating the acceptors [38, 39]. This is the reason that reports for N doped ZnO (NZO) film produced using an N_2 source led to n-type, and not p-type conduction [40, 41]. Table 2.1 shows the chemical characteristics of the N molecules.

Table 2.1 Chemical properties for N_2, N_2O, NO, and NO_2 molecules. [37]

Characteristics of N molecules		Dissociation energy (eV)	Ionization energy (eV)	Thermal decomposition (℃)
N_2	Neutral	D(N–N) = 9.60	15.58	>1000
N_2O	Neutral	D(N_2 –O) =1.65 D(NO–O) = 4.93	12.89	>260
NO	Radical	D(N–O) = 6.50	9.26	>700
NO_2	Radical	D(NO–O) = 3.51	9.78	>150

In recent years, there are numerous reports on the realization of p-type using N as dopant by different approaches. Table 2.2 shows the electrical characteristics of NZO thin films grown by various techniques [13, 22, 42-53]. However, most of the reports showed that single N doped ZnO is considered resistive for the practical used in optoelectronic devices.

Co-doping approach (simultaneous doping of donor and acceptor) that can enhance acceptor solubility and improve the p-type conductivity for ZnO has been theoretically proposed by Yamamoto and Yoshida based on ab initio electronic band structure calculations [54]. The model proposed that formation of acceptor-donor ions pairs can reduce the Mandelung energy (work done for the system of ions to be excited to higher energy). The Mandelung energy was found to decrease with group III elements (Al, Ga, In) for n-type doping and increase with group V element (N) for p-type doping. Consequently, many experimental studies have been carried out actively based on this approach by using N as acceptors and Al, Ga or In as donors [55-58]. Among the group III element, Al is more suitable due to its high stability to form bond with N or O, and because of its lowest Mandelung energy among the three [59]. The electrical properties of aluminium-nitrogen codoped ZnO (ANZO) thin films prepared by different growth approach are shown in Table 2.3 [60-75].

Table 2.2 Electrical characteristics of NZO thin film with different growth technique and condition.

Growth technique	film source	dopant source	Thermal treatment (℃)	Electrical properties				References
				conduction type	resistivity, ρ (Ω.cm)	carrier concentration, n (cm^{-3})	mobility, μ (cm/V.s)	
P-MBE	Zn	NO	T_s = 400	p	9.4	1.3×10^{18}	0.5	[42]
		N_2/O_2	T_s = 400	n	4.9×10^{2}	1.4×10^{16}	0.9	
ECR assist PLD	ZnO	N_2/O_2 = (15/85)%	T_s = 630	p	3.0×10^{1}	5.0×10^{17}	0.9	[43]
PEMOCVD	Zn	NO	T_s = 250	p	3.3×10^{2}	6.1×10^{16}	0.3	[44]
		N_2O	T_s = 250	p	1.7×10^{4}	3.9×10^{14}	1.0	
	Zn	N_2O/O_2	T_s = 430	p	8.7	3.4×10^{17}	2.1	[22]
	Zn	N_2O/O_2	T_s = 450	p	2.3×10^{1}	9.0×10^{16}	3.0	[45]
MOCVD	Zn	NO/O_2	T_s = 400	p	1.6×10^{1}	1.2×10^{17}	3.3	[46]
	Zn	NH_3/O_2	T_s = 600	p	2.3×10^{1}	1.3×10^{17}	2.2	[13]
	Zn	N_2O/O_2	T_s = 400	p	$\sim 10^{-1}$	$\sim 10^{18}$	320.0	[47]
RF sputtered	ZnO	NO/Ar = (70/30)%	T_s = 500	p	3.5	2.4×10^{18}	0.7	[48]
	ZnO	N_2/Ar = (23/77)%	T_s = RT	p	3.2	1.3×10^{19}	0.1	[49]
	ZnO	N_2/Ar = (10/90)%	T_s = RT	p	1.9×10^{2}	1.3×10^{14}	257.0	[50]
		N_2/Ar = (25/75)%	T_s = RT	p	5.6	5.2×10^{16}	22.0	
		N_2/Ar = (75/25)%	T_s = RT	n	5.5×10^{1}	-	4.6	[51]
	ZnO	N_2/Ar = (25/75)%	T_s = RT	p	1.5×10^{3}	2.6×10^{15}	2.0	[52]
		N_2/Ar = (75/25)%	T_s = RT	p	7.9×10^{2}	3.6×10^{14}	22.0	
	ZnO	N_2/O_2 = (60/40)%	T_s = 450	p	7.2×10^{1}	9.5×10^{14}	91.5	[53]

Table 2.3 Electrical characteristics of ANZO thin film with different growth technique and condition. (cont.)

Growth technique	Source	dopant	Thermal treatment (℃)	Electrical properties				References
				conduction type	resistivity, ρ (Ω.cm)	carrier concentration, n (cm^{-3})	mobility, μ (cm/V.s)	
USP	Zn = (1)	N/ Al = (3:0.05)	T_s = 400	p	1.7×10^{-2}	5.1×10^{18}	73.6	[60]
	Zn = (1)	N/ Al = (3:0.15)	T_s = 450	p	3.3	4.6×10^{18}	0.4	[61]
sol gel	Zn = (1)	N/ Al = (1:0.01)	T_s = RT	p	1.9×10^{1}	2.0×10^{17}	1.6	[62]
DC sputtered	Zn doped 1wt% Al	NH_3/O_2 = (15/85)%	T_s = 450	p	1.6×10^{2}	5.6×10^{17}	0.1	[63]
	Zn doped 0.01at% Al	NH_3/O_2	T_s = 480	p	3.1×10^{2}	5.7×10^{17}	0.4×10^{-1}	[64]
	Zn doped 0.15wt% Al	N_2O	T_s = 500	p	5.7×10^{1}	2.5×10^{17}	0.4	[65]
	Zn doped 0.4at% Al	N_2O	T_s = 500	p	5.5×10^{1}	1.3×10^{18}	0.1	[66]
RF sputtered	ZnO	AlN; Ar	T_s = RT	p	5.3×10^{-1}	5.0×10^{18}	2.4	[67]
	ZnO	AlN; N_2/Ar = (4:96)%	T_s = RT	p	3.9	1.2×10^{18}	1.4	[68]
	ZnO	AlN; O_2/Ar	T_s = 450	p	5.5×10^{-1}	3.8×10^{19}	0.3	[69]
	Zn	Al; N_2/O_2 = (40:60)%	T_s = 300	p	1.9×10^{-2}	2.9×10^{19}	-	[70]
	ZnO	Al; N_2/O_2	T_s = 300	p	2.0×10^{-2}	2.7×10^{19}	12.4	[71]

	ZnO	Al; $N_2/O_2/Ar$	T_s = 600	p	1.3×10^{-2}	3.0×10^{18}	154.0	[72]
	ZnO doped 2wt% Al_2O_3	N_2/Ar = (75:25)%	T_s = RT	p	2.1×10^{1}	7.8×10^{17}	0.5	[73]
	ZnO doped Al_2O_3	N_2O/Ar	T_s = 500	p	2.6	2.5×10^{17}	9.6	[74]
	ZnO doped 1.5wt% Al_2O_3	N_2O/Ar = (25:75)%	T_s = 500	p	-	2.3×10^{17}	-	[75]

2.2 Thin film growth technique

Thin film can be a single layer or multi-layer of insulator, conductor or semiconductor on substrate. ZnO which is an II-IV semiconductor can be easily deposited in the form of thin films by various techniques such as pulse laser deposition (PLD) [76], metal organic chemical vapour deposition (MOCVD) [77], molecular beam epitaxial (MBE) [78], electrochemical growth [79], ultrasonic spray pyrolysis (USP) method [80] and sputter deposition [81-83].

2.2.1 Sputter deposition: Radio frequency (RF) magnetron sputtering

Sputter deposition is a physical vapour deposition (PVD) process that is widely used in the semiconductor industry. The general mechanism for sputtering involves the gas ions bombardment (normally from inert gas such as Ar) to excite the source materials (target) and depositing it in the form of thin film on a substrate. In a vacuum chamber, there is an applied negative charge on the target which causing a plasma, where it attracts the positively charged gas ions at a very high speed. This collision creates a momentum transfer and ejects atomic particles from the target surface. The electrode (cathode) utilized strong electric and magnetic fields to trap electrons close to the surface. Hence, it increases the probability of number of electrons striking the Ar atoms, such that the ionization efficiency is significantly higher. [84]

There are mainly two types of magnetron sputtering system, which are direct current (DC) and radio frequency (RF) modes. The main difference between the two is the type of power applies in creating the potential difference between the anode and cathode. In DC sputtering, a direct voltage will be applied which is beneficial for

the deposition of conducting material at a high rate. If the target is less or non-conducting material, positive charges will build up on the target, which will then decrease the potential difference between anode-cathode and influences the sputtering rate. Build up charges can be avoided by the use of RF sputtering, where the alternating potential controlled by the radio frequency generator will vary the sign of the anode-cathode bias at a high rate. Hence, RF sputtering is useful to sputter a wide range of conductive, semiconductor and insulator materials. The difference in schematic diagram between the DC and RF sputtering is shows in Figure 2.1.

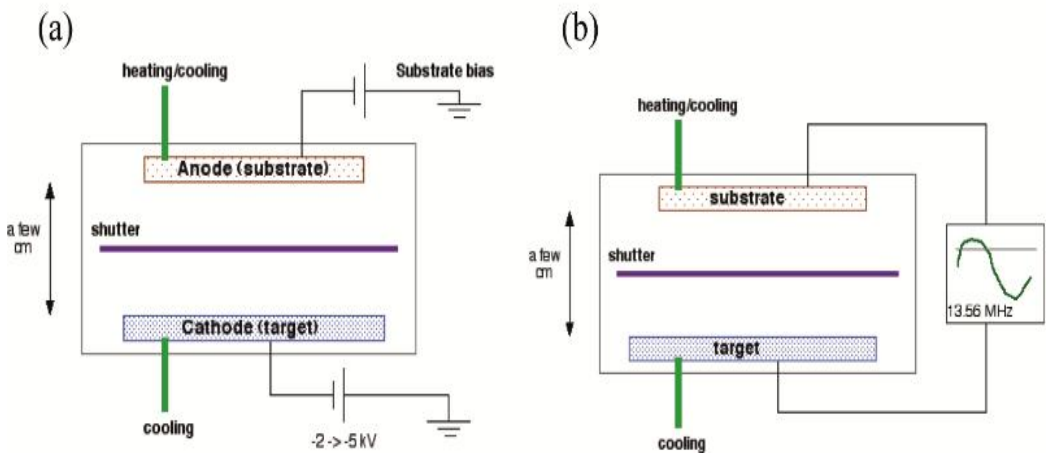

Figure 2.1 Schematic diagrams of (a) DC and (b) RF modes sputtering. [85]

The advantage of RF magnetron sputtering is well known such as high quality thin film with uniform thickness, good adhesive and highly c-axis oriented thin film can be prepared with lower cost, simplicity and lower substrate temperature.

2.3 Metallization

Thermal evaporator involves the condensation of the heated and melted source on the substrates which take place in a high vacuum. Basically, electric resistance heater (heating filament) is used to melt the source material and raise the vapour pressure inside the vacuum chamber. The vacuum allows the vapour (evaporated particles at the bottom part) to travel directly on the substrate (top part) by reducing the collision or scattering. Good vacuum plays an important role to reduce the impurity, control the uniformity and thickness of the deposited film. However, it is important to take precaution on the shadowing/step coverage because evaporated materials condense on the substrate mostly from a single direction where protruding features block the evaporated material from some areas. Furthermore, only materials with a much higher vapour pressure than the heating element can be deposited to prevent contamination of the film. It is common to use this technique for the metallization of the metal contact due to the simplicity, fast deposition rate and large coverage area. [86, 87]

2.4 Electrical properties components

The bulk resistivity (ρ), carrier concentration (n), and carrier mobility (μ) are the basic components for electrical properties of a material. A material can be distinguished as an insulator, semi-insulator, semiconductor or conductor according to their bulk resistivity. Table 2.4 demonstrates various categories of material with respect to their bulk resistivity.

Table 2.4 Different material categorized by its bulk resistivity range [88].

Material categories	Range of bulk resistivity (Ω.cm)
Insulator (dielectric)	10^{10} - 10^{22}
Semi-insulator	10^{3} - 10^{10}
Semiconductor	10^{-4} - 10^{3}
Conductor	10^{-6} – 10^{-4}

2.4.1 Metal-semiconductor interface

Metal-Semiconductor interface (or contacts) brings the metal and semiconductor together. It can be categorize as Ohmic (non-rectifying) or Schottky (rectifying) behavior depending on the barrier height form in the interface of metal-semiconductor. Difference in work functions of metal, ϕ_m and semiconductor work function, ϕ_s after they are brought in contact contribute significantly to the barrier heights. The band gap, the type of dopant and its concentration in the semiconductor also affect the behavior of the junction.

Ohmic contact is a two directional carrier flow system, where the barrier height in metal-semiconductor interface is small and the carriers can flow across it easily. A linear and symmetric current-voltage (*I-V*) relationship under both positive and negative voltage will be obtained. The carrier transport mechanisms involved in ohmic contact are tunneling effect (the probability of the low energy particles to penetrate through the potential barrier) and field emission (the high energy particles to overcome the potential barrier). [89, 90]

Chemical reaction between metal and semiconductor, interface traps and defects, surface states, impurities and diffusion of the metal into the semiconductor are the main reasons in the forming of Schottky contact. When the barrier height in metal-semiconductor interface is high, the carrier transport mechanism at the contacts is

known as thermionic emission. This will result in rectifying *I-V* relationship that similar to the diode, where most of the carrier can only flow under positive voltages but almost no carrier can flow under negative voltages. Hence, Schottky contact is one directional carrier flow system. [91]

Practically, the presence of extrinsic surface states such as oxides and defects can make the behavior of the contact almost independent of the difference in work function and electron affinity [92]. Hence, the contact region is doped externally in order to create an extrinsic layer and ensure the type of contact required in semiconductor device fabrication. The ohmic and rectifying *I-V* curves are shown in Figure 2.2.

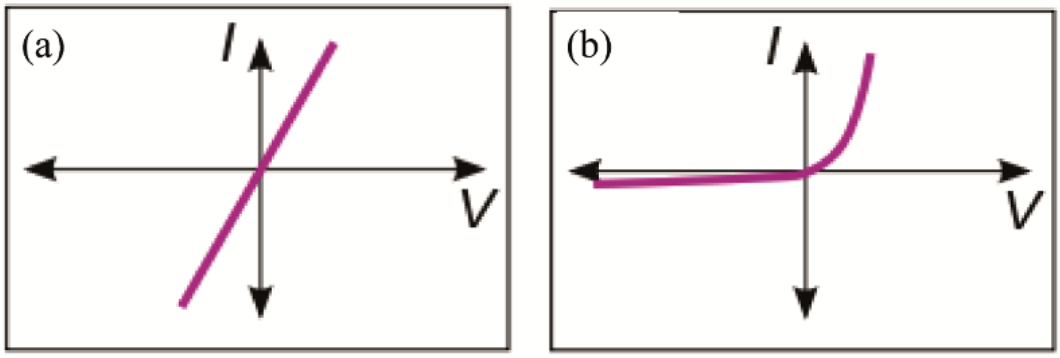

Figure 2.2 Metal-semiconductor interface behavior represented by *I-V* characteristics. (a) Ohmic contact and (b) Schottky contact. [93]

2.4.2 Metal-Oxide-Semiconductor (MOS) capacitor

Metal-Oxide-Semiconductor (MOS) capacitor is a structure where an oxide is placed between a semiconductor and a metal gate. Fundamentally, the semiconductor and the metal gate are the two plates of the capacitor and the oxide functions as the dielectric. The basic structure of a MOS is shown in Figure 2.3.

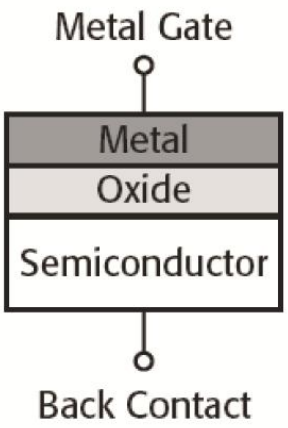

Figure 2.3 The basic components of MOS capacitor structure. [94]

Capacitance-voltage (*C*-*V*) measurements are commonly used to analyse the MOS devices. The capacitance of the MOS structure depends on the DC voltage (bias) applied on the metal gate where 3 regimes of operation exist in MOS capacitor are accumulation, depletion and inversion. Flatband voltage (V_{FB}) is the voltage at which there is no charge on the plates of the capacitor and hence there is no electric field across the oxide. It divides the accumulation regime from the depletion regime. Threshold voltage (V_T) is the gate voltage at which the inversion layer started to be formed. It separates the depletion regime from the inversion regime [95]. The regimes of MOS operation for an n-type semiconductor (pMOS) are presented clearly by *C*-*V* curve (Figure 2.4).

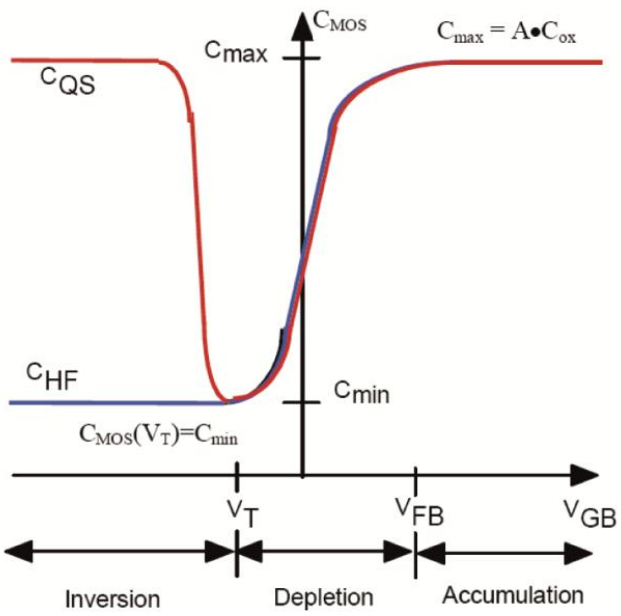

Figure 2.4 The metal gate DC voltage (V_{GB}) dependent *C-V* curves of a pMOS, where C_{HF} is high frequency capacitance and C_{QS} is quasi-static or low frequency capacitance. [95]

When no voltage applied on metal gate, an n-type semiconductor has majority mobile electrons. Accumulation occur typically when a positive voltages bias ($V_{GB} > V_{FB}$) is applied, the positive charge on the metal gate attracts mobile electrons from the semiconductor to the oxide-semiconductor interface. When negative bias ($V_T > V_{GB} > V_{FB}$) is applied to the gate metal, the negative charge near the gate-oxide interface induced positive charges near the oxide-semiconductor interface which will then push the mobile electrons away. The semiconductor is now depleted of mobile carriers and left behind positive space charge (depletion) region. When a more negative bias ($V_{GB} > V_T$) is applied, the number of majority electrons decreases while the number of minority holes increased nears the oxide-semiconductor interface. Therefore a positively charged inversion layer exists in addition to the depletion region near the oxide-semiconductor interface. The mechanism involved in p-type semiconductor (nMOS) is vice-versa. [96]

The MOS capacitor is one of the most suitable device to investigate the electrical properties. It has superior advantages such as non-destructive (without destroying the samples), simplicity in fabrication and analysis, effective even on highly compensated/intrinsic samples. The semiconductor conductivity type can be determined easily from the high frequency *C*-*V* curve measured on MOS capacitor due to its asymmetry and regardless of its interface charge density or polarity. The parameters, such as oxide thickness (t_{ox}), V_{FB}, V_T, space charge concentration (N_a), etc., can be extracted from the *C*-*V* data.

The oxide capacitance (C_{ox}) is the high frequency capacitance when the device is biased for strong accumulation and acts like a parallel-plate capacitor. For a relatively thick oxide (>50 Å), t_{ox} may be calculated from C_{ox} and the gate area (*A*) using the following equation [94]:

$$t_{ox} = \frac{(10^7) A \varepsilon_{ox}}{C_{ox}} \tag{2.1}$$

where t_{ox} is the oxide thickness (nm), *A* is the gate area (cm^2), ε_{ox} is the permittivity of the oxide material (F/cm), C_{ox} is the oxide capacitance (F) and 10^7 for unit conversion from cm to nm.

The N_c and N_v is the effective density of states in conduction and valence band respectively and given by Nicollian et al. [97]

$$N_c = 12 \times \left(\frac{2\pi m_0 m_e k_B T}{h^2}\right)^{\frac{3}{2}}, \qquad N_v = 2 \times \left(\frac{2\pi m_0 m_h k_B T}{h^2}\right)^{\frac{3}{2}} \tag{2.2}$$

where h is the Planck constant, k_B is Boltzmann constant, m_0 is the electron rest mass, m_e = 0.28 and m_h = 0.58 is the effective electron and hole mass for ZnO [98].

The intrinsic carrier concentration (cm^{-3}), n_i can be calculated from N_c and N_v by the following equation [99]

$$n_i = (N_c N_v)^{\frac{1}{2}} . \exp(\frac{-E_g}{2k_B T}) \tag{2.3}$$

where k_B is the Boltzmann constant, T is the temperature (Kelvin), E_g is the energy band gap for ZnO which is 3.27 eV in this case.

The N_a (cm^{-3}) for the MOS is obtained by the iteration method that fulfilling the following condition by using maximum-minimum capacitance method [97]

$$\frac{N_a}{\ln(\frac{N_a}{n_i}) + \frac{1}{2}\ln[2\ln(\frac{N_a}{n_i}) - 1]} = (\frac{4k_B T \varepsilon_{ox}{}^2}{q^2 \varepsilon_s t_{ox}{}^2}).(\frac{C_{ox}}{C_{\min}} - 1)^{-2} \tag{2.4}$$

where ε_s (F/cm) is the permittivity of the semiconductor material, $C_{\min}$ (F) is the minimum capacitance and n_i is the intrinsic carrier concentration. The example for iteration method in obtaining N_a can be referred to Appendix (A).

2.5 Characterization technique

2.5.1 Van der Pauw method

The bulk resistivity of the semiconductor is often determined using a four-point probe technique where two of the probes are used to source current and the other two probes are used to measure voltage. Measurement errors due to the probe resistance, spreading resistance and the contact resistance can be eliminated using a four probe measurement due to the use of a high impedance voltmeter. There are two modes of four point probe method which are four point collinear probe method and Van der Pauw method, where the main difference between the two is the contacts placement. [100]

The Van der Pauw method is useful for measuring simple and small geometric samples with the geometrical contact spacing is irrelevant. However, the measurements take long time and require precaution in samples preparation and measurement. Details of samples preparation and the conditions stated below must be fulfilled to avoid the geometrical error. [101, 102]

- Contact placement must be on the circumference of the sample.
- Contacts size must be sufficiently small.
- The sample is of uniform thickness,
- The sample is singly connected (contains no isolated holes).

Figure 2.5 shows the types of Van der Pauw geometrical samples. Square shape sample is most commonly used due to its simple preparation but error introduced is quite large. With the geometry sample length, L and contact length of c in the ratio of c/L < 0.1, the measurement error introduced is less than 10%. The Greek cross sample with the geometry ratio of L/w > 1.02 introduced less than 1% error where the four arms serve to isolate the contacts from the active region. [101]

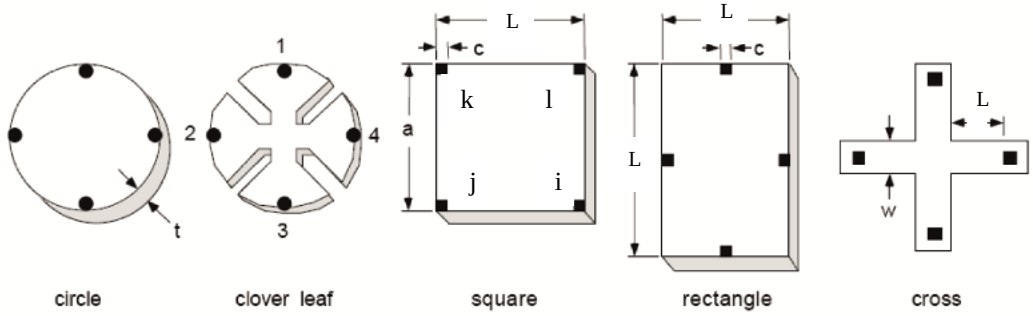

Figure 2.5 Van der Pauw samples with various geometry shapes. [101]

A DC current I when applied to the sample should yields the power dissipation of not exceeding 5 mW (preferably 1 mW) and given as

$$I = (200R)^{-0.5} \tag{2.5}$$

where R is the resistance measured between two opposing lead.

The Van de Pauw resistivity, ρ can be obtained by measuring the potential difference (V) parallel to the circumference of the square samples [100]

$$\rho = \frac{\pi t_s}{\ln 2} f \frac{(V_{ji,kl} - V_{ij,kl} + V_{kj,li} - V_{jk,li})}{4I} \tag{2.6}$$